

Surface Tension of the 3-Dimensional Lennard-Jones fluid from Histogram-Reweighting Monte Carlo Simulations.

Jeffrey J. Potoff*

Department of Chemistry and Department of Chemical Engineering and Materials Science, University of Minnesota, Minneapolis, MN 55455-0431

Athanasios Z. Panagiotopoulos

Institute for Physical Science and Technology and Department of Chemical Engineering, University of Maryland, College Park, MD 20742-2431

(December 25, 1999)

The surface tension of the full 3-dimensional Lennard-Jones potential is calculated from grand canonical Monte Carlo simulations with the finite-size scaling methodology outlined by Binder [Phys. Rev. A. **25**, 1699 (1982)]. Surface tensions are determined for the range of reduced temperatures $T^* = 0.95 - 1.312$ and are found to be in good agreement with molecular dynamics calculations. A critical temperature $T_c^* = 1.311 \pm 0.002$ is established by locating the T^* where the surface tension of the infinite system size vanishes. In addition, with this method it is possible to determine the critical exponent 2ν . For the Lennard-Jones fluid we found $2\nu = 1.42 \pm 0.08$, which differs from the accepted value of $2\nu = 1.26$.

I. INTRODUCTION

Due to the importance of the surface tension, γ on the behavior of fluids and fluid mixtures, it has been studied extensively over the last century. The earliest modern theory of surface tension is given by van der Waals [1]. By replacing the classical equation of state originally used by one that reproduced thermodynamic singularities at the critical point, Fisk and Widom were able to make predictions of the surface tension near the critical point [2]. Later it was determined that separate universal ratios should exist between γ_0 , which characterizes the vanishing of the surface tension in the critical region, and ξ_0 , which characterizes the divergence of the correlation length, and between γ_0 and each of the amplitudes characterizing the divergence of the specific heat per unit volume [3]. As a result, the measurement of the surface tension, correlation length or specific-heat divergence leads to knowledge of all three quantities [4].

In addition to theoretical treatments and experiment, many simulation studies have been performed to calculate the surface tension of the liquid-vapor interface for simple potential models. The calculation of surface tensions from simulation is considerably more complex than phase coexistence calculations. Methods for directly calculating phase coexistence properties, such as Gibbs ensemble Monte Carlo [5–7], are effective primarily because they *avoid* the formation of a liquid-vapor interface. Since no interface is formed in Gibbs ensemble simulations, they cannot be used for the determination of properties of the interface. Instead, NVT Monte Carlo [8–11] and molecular dynamics [12–18] techniques have been used for surface tension calculations. The predictions of these

studies for the surface tension of the Lennard-Jones potential are widely scattered and depend on method, system size, potential cutoff radius and run length [19].

Histogram-reweighting techniques [20,21] provide accurate data for the free energy of a system over a range of thermodynamic conditions, including the interface region. Binder has suggested a method for calculating the surface tension by examining the finite-size scaling behavior of the ordering operator distribution [22], which is readily available from grand canonical Monte Carlo simulations. This method avoids the need to establish an interface profile and is especially attractive for use in the critical region. To this date, this method has been applied to a variety of lattice models, including 2D [22–24] and 3D [22,24] Ising models and Potts [25–27] models. Application to continuum models has been limited an NpT ensemble study of the Lennard-Jones potential [28].

In this work, we use grand canonical histogram-reweighting Monte Carlo simulations to calculate the surface tension of the full Lennard-Jones potential for a range of temperatures. In section II we describe how the surface tension is determined for a finite system and the finite-size scaling analysis used to extrapolate these results to the infinite system size. The details of the Monte Carlo simulations are given in section III. The results of our surface tension calculations are in section IV. Finally, the conclusions of this work can be found in section V.

*To whom correspondence should be addressed. Electronic mail: potoff@chem.umn.edu

II. METHODOLOGY

The probability of observing a certain number of particles N is defined as $P(N)$. At the point of phase coexistence, this distribution becomes bimodal, with separate peaks of equal area for the liquid and vapor phases. The free energy of the interface for a finite system, shown in Figure 1, is given by:

$$F_L = \ln(P(N_{max})) - \ln(P(N_{min})), \quad (1)$$

where $P(N_{max}) = (P(N_{max}^{vap}) + P(N_{max}^{liq}))/2$ is the average of the liquid and vapor peak heights and $P(N_{min})$ is the minimum between the liquid and vapor peaks.

According to Binder, in the limit of large L we can write [22]:

$$P(N_{min}) = AL^x \exp(2L^{d-1}F_s/k_bT), \quad (2)$$

where F_s is the interface free energy for the infinite system and L is the length of the simulation cell. The pre-exponential factor A and exponent x are unknown. While it is not possible to calculate F_s directly, it is possible to calculate the interface free energy for a range of system sizes and extrapolate the results to the infinite system size according to [22,28]:

$$\beta\gamma_L = \frac{\beta F_L}{2L^{d-1}} = \beta\gamma - \frac{x \ln L}{2L^{d-1}} - \frac{\ln A}{2L^{d-1}}. \quad (3)$$

The reciprocal temperature $\beta = 1/k_B T$, γ_L is the surface tension of the finite-size system and $\gamma = F_s/2L^{d-1}$ is the surface tension of the infinite system. The factor of 2 in the denominator of the expression for γ arises from periodic boundary conditions.

Near the critical point the simulation fluctuates readily between liquid and vapor phases. As the temperature is lowered, the free energy barrier between phases increases to the point where there is a vanishingly small probability that the simulation will fluctuate between phases. This is especially problematic in this case, since configurations in the interface region are necessary for accurate calculations of the surface tension. To circumvent the problems of sampling the interface region at lower temperatures, the multicanonical method of Berg and Neuhaus [25] is used.

The multicanonical ensemble method overcomes the large free energy barrier between phases at low temperatures by artificially enhancing the probability of the simulation making a transition from one bulk phase to the other. This improvement is achieved by sampling from a non-physical distribution $\pi(N)$ instead of the physical distribution $P(N)$. The N particle distribution in the multicanonical ensemble $\pi(N)$ is related to the grand canonical $P(N)$ through an arbitrary weighting function $g(N)$:

$$\pi(N) = g(N)P(N) \quad (4)$$

From equation 4 it is apparent that $g(N) = 1/P(N)$ yields a constant $\pi(N)$. To implement $g(N) = 1/P(N)$ as the weighting function, however, $P(N)$ must be known to a reasonable accuracy. Estimates of $P(N)$ can be determined by reweighting $P(N)$ from other conditions to the conditions of interest, such as from high temperatures to lower temperatures or by performing short exploratory simulations. Once $g(N)$ is known, a multicanonical simulation can be performed. The outcome of which is a nearly flat N particle histogram $\pi(N)$. The improved grand canonical $P(N)$ distribution is recovered from $\pi(N)$ by dividing out the weighting factor $g(N)$:

$$P(N) = \frac{\pi(N)}{g(N)} \quad (5)$$

The methods of entropic sampling [29] and expanded ensembles [30] are closely related to the multicanonical ensemble technique.

III. MONTE CARLO SIMULATIONS

We study the surface tension of particles that interact through a Lennard-Jones potential:

$$U(r_{ij}) = 4\epsilon_{ij} \left[\left(\frac{\sigma_{ij}}{r_{ij}} \right)^{12} - \left(\frac{\sigma_{ij}}{r_{ij}} \right)^6 \right] \quad (6)$$

where U is the configurational energy of pair interaction, r_{ij} is the distance between particles i and j and ϵ_{ij} , σ_{ij} are potential parameters for the ij interaction. In this work $\sigma_{ij} = \epsilon_{ij} = 1.0$. The total energy of system is assumed to be pairwise additive. Three-body and higher order terms are not included in the energy calculation. Variables are reduced as follows: the temperature $T^* = k_B T/\epsilon$, the density $\rho^* = N\sigma^3/V$, and the surface tension $\gamma^* = \gamma\sigma^2/\epsilon$.

Truncation of the potential has a strong effect on the phase behavior and critical properties [31]. The surface tension has also been shown to be strongly affected by truncation of the potential [19]. In this study we use the full (non-truncated) potential. Long-range corrections were performed with the method of Theodorou and Suter [32]. The advantage of this method is that corrections to the energy are significantly smaller than when the potential is cut at $L/2$ and tail corrections are added.

Estimates of the surface tension for $T^* = 1.26 - 1.3120$ were extracted from the histograms collected in the study of the Lennard-Jones critical point. Details of these simulations are given in [33]. The data for the $V = 343$ system size were found to lie outside the finite-size scaling regime and were not used in the extrapolations to find $\gamma^*(L = \infty)$.

For temperatures lower than $0.95T_c^*$ it was necessary to employ multicanonical sampling techniques [25] to gather accurate statistics in the interface region. Simulations

were performed for the $V = 512, 729, 1000$ and 1728 system sizes at $T^* = 1.127, 1.05$ and 1.00 . Simulations varied in length from 250 million Monte Carlo steps (MCS) for the $V = 512$ system size to 1 billion MCS for the $V = 1728$ system size. Histogram data of N and E were collected every 250 MCS to every 1000 MCS depending on system size. Weighting functions for the multicanonical simulations were determined by reweighting data collected near the critical point to the temperature of interest. The resulting $P(N)$ distribution was then inverted and used as the weighting function. In order to improve the temperature range over which the multicanonical histograms could be reweighted, additional liquid phase simulations of 50 million MCS were performed at $T^* = 0.95$ for the $V = 512$ system, while it was necessary to perform liquid-phase simulations for $T^* = 0.95, 1.00$ and 1.05 for the $V = 1728$ system. Additional liquid-phase simulations were also performed for intermediate system sizes. These standard GCMC histogram-reweighting simulations were patched with the multicanonical simulation data according to the method outlined in [33].

Statistical uncertainties were determined by performing 3 independent sets of simulations with different random number seeds. The standard deviation of the results from the three simulation sets was used as the statistical uncertainty estimate.

IV. RESULTS AND DISCUSSION

We begin our study by investigating the free energy barrier height βF as a function of $1/L$. In Figure 2, βF is plotted versus $1/L$. For $T^* = 1.312$, we find that the barrier height is independent of system size, verifying earlier predictions of $T_c^* = 1.3120(7)$ calculated with mixed-field finite-size scaling techniques [33]. Below the critical temperature, the data display the appropriate increase in the barrier height with system size.

In Figure 3, $\beta\gamma_L = \beta F_L/2L^2$ is plotted versus the scaling variable $\ln(L)/L^2$ for temperatures near the critical point. As shown in the figure, the data display clearly the expected linear behavior. Extrapolation to $L = \infty$ yields $\beta\gamma^*$ for the infinite system size. The results of these extrapolations are given in Table I. At the critical point, the surface tension is expected to vanish. Extrapolation of the data for $T^* = 1.312$ yields $\gamma^* = -0.0005(2)$, while extrapolation of the data for $T^* = 1.310$ results in $\gamma^* = .0001(3)$. This suggests that the critical temperature lies between $T^* = 1.312$ and 1.31 , which verifies our predictions of the surface tension are consistent with the expected critical behavior.

In addition, we compare our results with those of a similar study where simulations were performed in the NpT ensemble for $N = 32, 108, 256$ and 500 Lennard-Jones particles [28]. For the $N = 256$ and $N = 500$ system sizes, the agreement of the data of [28] with our work is good, as shown by Figure 3. For the smaller

$N = 32$ and $N = 108$ system sizes, the data of Hunter and Reinhardt (not shown) are not in good agreement with our predictions. The large degree of curvature seen when including the $N = 32$ and $N = 108$ data in the plot of $\beta F_L/2L^2$ versus $\ln(L)/L^2$ suggests that these system sizes lie outside the finite-size scaling regime where this method is valid.

From hyperscaling relations, the surface tension is expected to vary as $\gamma = \gamma_0(1 - T/T_c)^{2\nu}$ in three dimensions [34]. A log-log plot of γ versus $1 - T/T_c$ can be used to extract an estimate for the critical exponent of the correlation length ν , as shown in Figure 4. By performing a linear regression on the data, we found $2\nu = 1.42(8)$, which differs significantly from earlier calculations of $2\nu = 1.91$ for the Lennard-Jones potential [28]. In comparison, Binder found $2\nu = 1.32$ for the 3D Ising model [22], which is closer to the accepted value of $2\nu = 1.26$ [35,36] and our result. It should be noted that the value of ν predicted from taking the slope of the $\ln\gamma$ versus $1 - T/T_c$ plot is drastically effected by small changes in the extrapolated surface tension at each temperature. Because the study of Hunter and Reinhardt was limited to small system sizes, their extrapolations may have significant errors that are magnified when attempting to calculate 2ν . To achieve better agreement with the work of Binder and theoretical predictions for ν , the simulation of larger system sizes, as well as longer runs to improve statistics, may be necessary.

Multicanonical sampling techniques were employed to determine the surface tension of the full Lennard-Jones potential for $T^* = 0.95, 1.0, 1.05, 1.1, 1.15$ and 1.20 . The surface tensions calculated for these temperatures are combined with the near T_c^* surface tensions and plotted vs T^* in Figure 5. Table I lists $\beta\gamma^*$ and the co-existence densities for each temperature studied. For comparison, we include recent molecular dynamics calculations of Mecke *et al.* [18]. For $T^* = 0.95 - 1.1$, the temperature range where the data overlap, there is good agreement between γ^* calculated by molecular dynamics and finite-size scaling.

In theory it would be possible to use this finite-size scaling methodology to determine surface tensions over the entire Lennard-Jones liquid-vapor phase diagram. In practice, however, the finite-size scaling technique is limited to temperatures relatively close to the critical temperature (in this case within $0.7T_c^*$). This is because the minimum in the density distribution $P(N_{min})$ rapidly goes to values on the order of 10^{-200} with decreasing temperature, while the peak height $P(N_{max})$ remains $O(0.1)$. The large free energy barrier between phases makes it difficult to construct biasing functions that are accurate enough for the multicanonical method to be effective. In addition, the need to simulate a number of different system sizes makes this method computationally prohibitive at low temperatures. For these reasons, the finite-size scaling method of Binder appears to be complementary to traditional molecular dynamics techniques for the calculation of surface tensions.

V. CONCLUSIONS

In this work, we have applied the finite-size scaling methodology of Binder [22] to calculate the surface tension of the full Lennard-Jones potential for a wide range of reduced temperatures. Near the critical point, our results are consistent with the expected critical behavior and verify the prediction of [33] for $T_c^* = 1.3120(7)$ within the error of the calculation. Our data in the critical region are also in good agreement with the work of Hunter and Reinhardt [28] who applied a similar finite-size scaling analysis to determine γ^* for the full Lennard-Jones potential from NpT ensemble simulations. At subcritical conditions, our results for γ^* for the full Lennard-Jones potential are in good agreement with the molecular dynamics calculations of [18]. For temperatures below $0.7T_c^*$, the calculation of surface tensions from finite-size scaling was found to be computationally prohibitive. This was due to both the need to simulate a range of system sizes and the difficulty in constructing the biasing functions necessary for the multicanonical method to be effective.

VI. ACKNOWLEDGMENTS

Research on which this manuscript is based was supported by the US Department of Energy, Office of Basic Energy Sciences, under grant DEFG02-98ER14C58. We would like to thank Lev Gelb for helpful discussions.

-
- [1] J. S. Rowlinson, *J. Stat. Phys.* **20**, 197 (1979).
 - [2] S. Fisk and B. Widom, *J. Chem. Phys.* **50**, 3219 (1969).
 - [3] D. Stauffer, M. Ferer, M. Wortis, *Phys. Rev. Lett.* **29**, 345 (1972).
 - [4] M. R. Moldover, *Phys. Rev. A* **31** 1022 (1985).
 - [5] A. Z. Panagiotopoulos, *Molec. Phys.* **61**, 812 (1987).
 - [6] A. Z. Panagiotopoulos, N. Quirke, M. Stapleton, and D. J. Tildesley, *Molec. Phys.* **63**, 527 (1988).
 - [7] B. Smit, Ph. de Smedt, and D. Frenkel, *Molec. Phys.* **68**, 931 (1989).
 - [8] K. S. Liu, *J. Chem. Phys.* **60**, 4226 (1974).
 - [9] J. K. Lee, J. A. Barker, and G. M. Pound, *J. Chem. Phys.* **60**, 1976 (1974).
 - [10] G. A. Chapela, G. Saville, and J. S. Rowlinson, *Faraday Discuss. Chem. Soc.* **59** 22 (1975).
 - [11] J. Miyazaki, J. A. Barker, and G. M. Pound, *J. Chem. Phys.* **64**, 3364 (1976).
 - [12] M. Rao and D. Levesque, *J. Chem. Phys.* **65**, 3233 (1976).
 - [13] G. A. Chapela, G. Saville, S. M. Thompson, and J. S. Rowlinson, *J. Chem. Soc. Faraday Trans. II* **8**, 1133 (1977).
 - [14] M. Rao and B. J. Berne, *Molec. Phys.* **37**, 455-61 (1979).
 - [15] J. P. R. B. Walton, D. J. Tildesley, and J. S. Rowlinson, *Molec. Phys.* **48**, 1357 (1983).
 - [16] M. Matsumoto and Y. Kataoka, *J. Chem. Phys.* **88**, 3233 (1988).
 - [17] M. J. P. Nijmeijer, A. F. Baker, and C. Bruin, *J. Chem. Phys.* **89**, 3789(1988).
 - [18] M. Mecke, J. Winkelmann, and J. Fischer, *J. Chem. Phys.* **107**, 9264 (1997).
 - [19] C. D. Holcomb, P. Clancy, and J. A. Zollweg, *Molec. Phys.* **78**, 437 (1993).
 - [20] A. M. Ferrenberg and R. H. Swendsen, *Phys. Rev. Lett.* **61**, 2635 (1988).
 - [21] A. M. Ferrenberg and R. H. Swendsen, *Phys. Rev. Lett.* **63**, 1195 (1989).
 - [22] K. Binder, *Phys. Rev. A* **25**, 1699 (1982).
 - [23] B. A. Berg, U. Hansmann, and T. Neuhaus, *Phys. Rev. B* **47**, 497 (1993).
 - [24] B. A. Berg, U. Hansmann, and T. Neuhaus, *Z. Phys. B* **90**, 229 (1993).
 - [25] B. A. Berg and T. Neuhaus, *Phys. Rev. Lett.* **68**, 9 (1992).
 - [26] A. Billoire, T. Neuhaus, and B. A. Berg, *Nucl. Phys. B* **B413**, 795-812 (1994).
 - [27] W. Janke, B. A. Berg, and M. Katoot, *Nucl. Phys. B* **B382**, 649 (1992).
 - [28] J. E. Hunter and W. P. Reinhardt, *J. Chem. Phys.* **103**, 8627 (1995).
 - [29] J. Lee, *Phys. Rev. Lett.* **71** 211 (1993).
 - [30] A. P. Lyubartev, A. A. Martsinovski, S. V. Shevkunov, and P. N. Voronotsov-Vel'yaminov, *J. Chem. Phys.* **96**, 1776 (1992).
 - [31] B. Smit, *J. Chem. Phys.* **96**, 8639 (1992).
 - [32] D. N. Theodorou and U. W. Suter, *J. Chem. Phys.* **82**, 955 (1985).
 - [33] J. J. Potoff and A. Z. Panagiotopoulos, *J. Chem. Phys.* **109**, 10914 (1998).
 - [34] B. Widom, *Phase Transitions and Critical Phenomena*, edited by C. Domb and M. S. Green (Academic, New York, 1972).
 - [35] A. M. Ferrenberg and D. P. Landau, *Phys. Rev. B* **44**, 5081 (1991).
 - [36] J. H. Chen, M. E. Fisher, and B. G. Nickel, *Phys. Rev. Lett.* **48**, 630 (1982).

TABLE I. Surface tension and coexistence densities for the full Lennard-Jones potential. Coexistence densities are from calculations of the $V = 2744$ system size for $T^* > 1.27$. For lower temperatures, a system size of $V = 512$ was used for coexistence density calculations. The number in parenthesis represents the statistical uncertainty in the last digit.

T^*	$\beta\gamma^*(L = \infty)$	ρ_{liq}^*	ρ_{gas}^*
1.312	-0.0004(3)	0.316(2)	0.316(2)
1.310	0.00006(3)	0.401(2)	0.236(2)
1.305	0.0015(3)	0.412(2)	0.225(2)
1.300	0.0033(4)	0.424(3)	0.213(2)
1.295	0.0053(4)	0.436(3)	0.202(1)
1.290	0.0077(4)	0.447(3)	0.191(1)
1.285	0.0103(5)	0.458(2)	0.182(1)
1.280	0.0136(7)	0.468(2)	0.173(2)
1.275	0.0154(8)	0.476(2)	0.166(2)
1.270	0.0194(8)	0.483(2)	0.160(2)
1.265	0.0240(9)	0.488(3)	0.154(3)
1.260	0.0288(9)	0.497(3)	0.149(1)
1.250	0.039(1)	0.509(2)	0.1415(2)
1.200	0.103(3)	0.564(1)	0.0996(2)
1.150	0.191(3)	0.605(1)	0.0739(6)
1.110	0.305(5)	0.642(3)	0.0550(2)
1.050	0.44(1)	0.672(3)	0.0404(1)
1.000	0.56(4)	0.701(1)	0.0294(2)
0.950	0.64(5)	0.730(3)	0.0210(1)

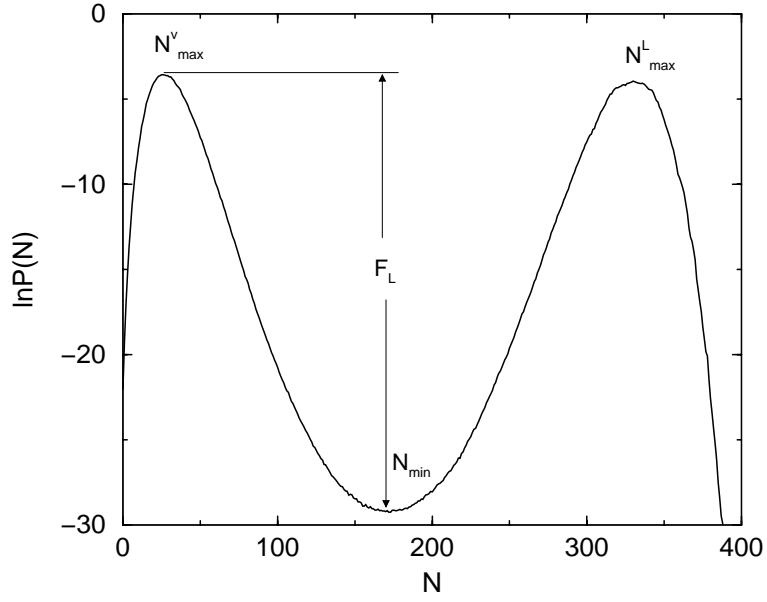


FIG. 1. Probability, $P(N)$ of observation of number of particles N for a system at $T^* = 1.10$, $V = 512$ and $\mu = -3.73$

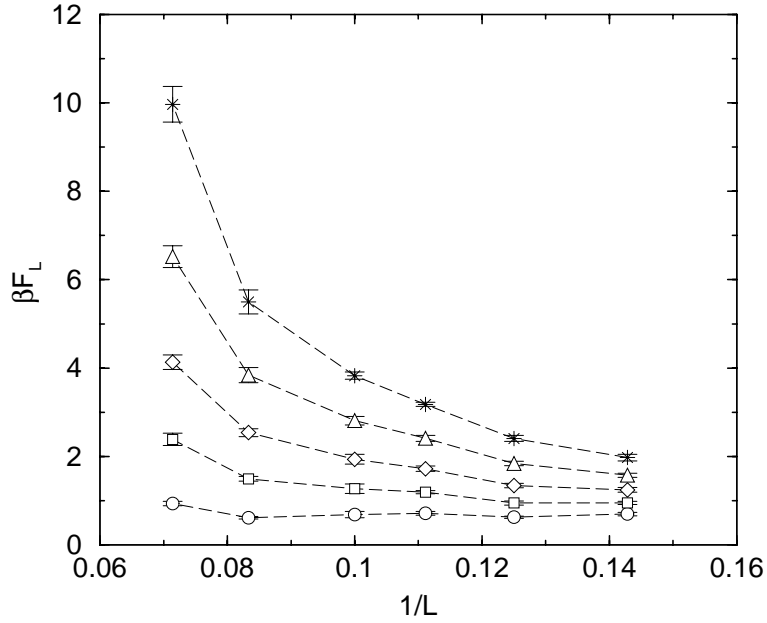


FIG. 2. L -dependence on the free energy barrier height for the full Lennard-Jones potential in the critical region. $T^* = 1.312$ (circles), $T^* = 1.30$ (squares), $T^* = 1.29$ (diamonds), $T^* = 1.28$ (triangles), $T^* = 1.27$ (crosses). The dashed line serves as a guide to the eye.

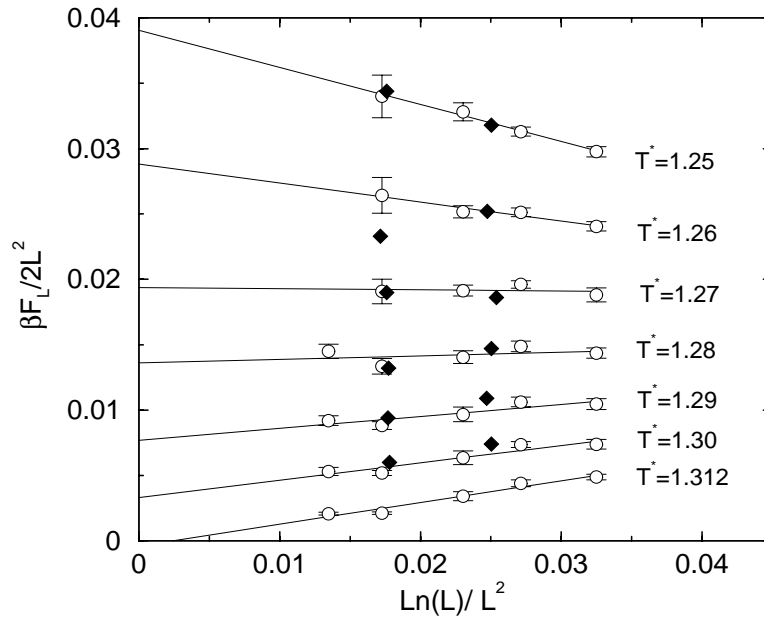


FIG. 3. L -dependence of the effective surface tension. This work(circles), NpT simulations (diamonds) [28]. The line represents a least-squares fit to the data.

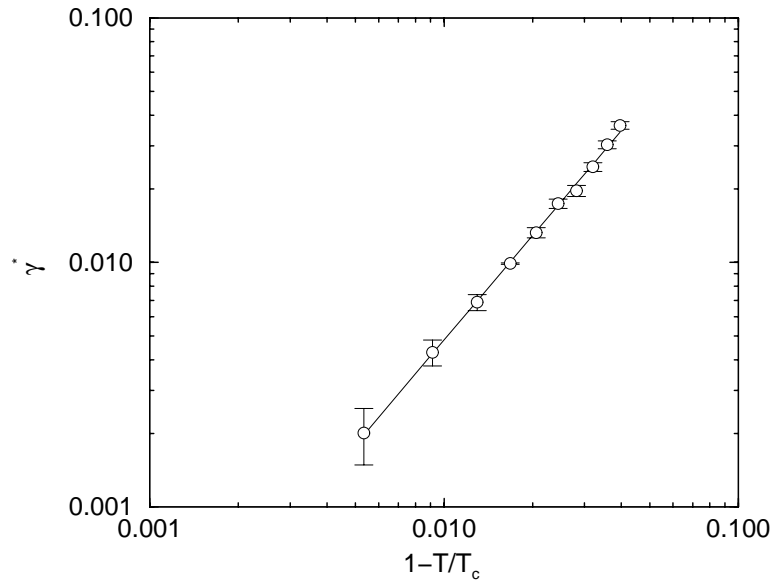


FIG. 4. Log-log plot of the surface tension of the Lennard-Jones fluid versus $1 - T/T_c$. Simulation data (circles). The line represents a least-squares fit to the data.

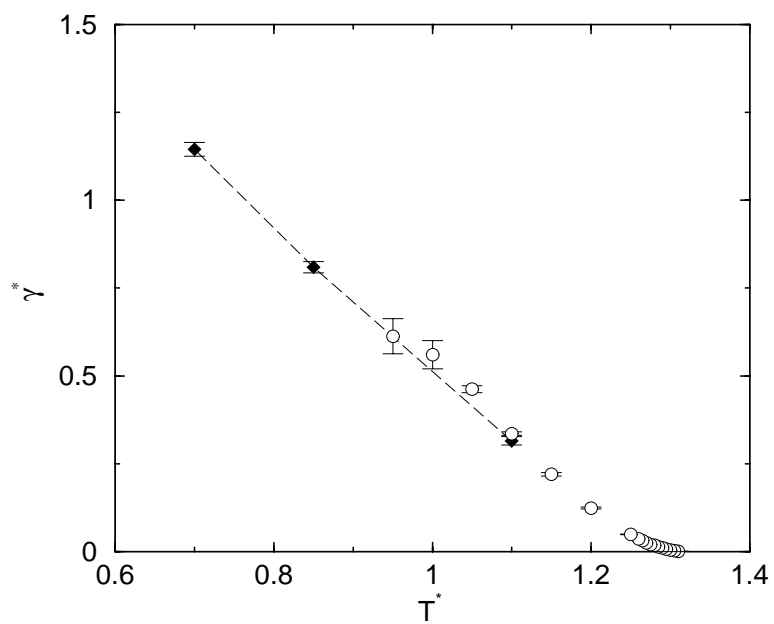


FIG. 5. The reduced surface tension of the Lennard-Jones potential versus T^* . This work(circles), the molecular dynamics calculations of Mecke *et al.* (filled diamonds) [18]. The dashed line serves as a guide to the eye.